

EUROPEAN ORGANIZATION FOR NUCLEAR RESEARCH

NP/Int/63-5  
12 August, 1963.

PARTICLE PRODUCTION IN PROTON-PROTON COLLISIONS AT 19 AND 24 GeV/c

A.N. Diddens, W. Galbraith\*, E. Lillethun, G. Manning\*, A.G. Parham\*,  
A.E. Taylor\*, T.G. Walker\*\*, and A.M. Wetherell

Summary

Cross sections for production of  $d$ ,  $\pi^+$ ,  $K^+$  and  $p^+$  have been measured at a laboratory angle of 116 mrad for  $p$ - $p$  interactions at 19 and 24 GeV/c. The observed spectra are compared with statistical model calculations. Significant cross sections were found for the production of deuterons of momenta in the range 2 - 9 GeV/c and with transverse momenta up to 1 GeV/c.

Introduction

Many measurements have been made on the production of particles in proton-nucleus interactions at energies of the order of 25 GeV, but little work has been carried out on the more fundamental  $p$ - $p$  production cross sections. In the course of the experiments on proton-nucleus collisions in this energy region several groups<sup>1-5</sup> have observed deuteron production. It is not clear whether the deuterons originated in proton-nucleon interactions or in proton-nucleus interactions. Appreciable deuteron yields were predicted by Hagedorn<sup>6</sup> in a calculation using a statistical model for  $p$ - $p$  interactions and by Butler and Pearson<sup>7</sup> using a cascade process from nuclei. Experiments performed by Amaldi et al<sup>8</sup>, Balea et al<sup>9</sup> and Schwarzschild and Zupančič<sup>5</sup> have supported production of deuterons of momentum less than 3 GeV/c in nuclear processes. At lower energies 2-3 GeV, however, deuteron production in  $p$ - $p$  interactions has been observed in hydrogen bubble chamber experiments<sup>10-12</sup>.

This paper reports yields of  $d$ ,  $\pi^+$ ,  $K^+$  and  $p^+$  at a production angle of 116 mrad from p-p interactions at 19 and 24 Gev/c. An external proton beam from the CERN proton synchrotron was used to bombard a liquid hydrogen target and the particles produced were identified by momentum analysis and velocity measurement using either a time-of-flight method or a differential Čerenkov counter.

### Experimental Details

An external proton beam was made by focusing protons scattered at an angle of about 20 mrad from a target placed in the internal beam of the synchrotron. The beam transport system and experimental arrangement are shown in Fig.1. Quadrupoles  $Q_1$  and  $Q_2$  were used to form an intermediate focus at the collimator C1 placed at the exit of the shielding wall. The beam size at this point was  $\sim 5$  cm diameter and the collimator C1 was 10 cm diameter. Momentum selection was obtained by a 40 mrad deflection in magnet M1. Previous analysis of a similar beam showed that at least 95% of the particles were protons in a 1 Gev/c band just below the internal beam momentum. The quadrupoles  $Q_3$  and  $Q_4$  were adjusted to focus this beam at the hydrogen target. The resulting beam size was 2 cm wide and 8 cm high. The collimator C2 was included to remove low intensity fringes from the beam and was positioned so that secondary particles from it were not detected by the counter telescopes.

An ion chamber of 15 cm diameter was placed between C2 and the hydrogen target. Ion chamber readings were taken for different distances between the ion chamber and the collimator to estimate the contribution to its readings from secondary particles produced in C2. At the position used for the ion chamber this contribution was less than 8%. The ion chamber and the associated current integrator were copies of that constructed and calibrated by Harting et al<sup>13</sup> and the calibration was checked by comparison using a strong  $\gamma$  ray source. The measured beam intensity was about  $7 \times 10^7$  protons for a circulating beam intensity of  $5 \times 10^{11}$  protons.

The hydrogen target used was 15 cm diameter and 100 cm long. Particles were detected by scintillation counter telescopes 1234 and 1567 defining a mean laboratory production angle of 116 mrad and spectrometer

magnet deflections of 192 and 292 mrad respectively. The momentum calibration of the spectrometer was made using a floating wire technique.

Particles detected by telescope 1234 passed through a gas Čerenkov counter<sup>14</sup> placed between scintillators 3 and 4. The Čerenkov counter was used as a differential counter with a velocity resolution of either 0.7% or 1.4%. Light collected outside the annular ring corresponding to this velocity band was used to give an anticoincidence signal to improve the rejection of particles with the wrong velocity. The momentum resolution of the counter telescope, 1234, had a full base width of about 20% and the solid angle from the target was  $3.6 \times 10^{-5}$  sr. Momentum scans were made with the spectrometer magnet for fixed values of the refractive index of the gas (ethylene) in the Čerenkov counter.

From the magnet settings found for the abundantly produced protons it was possible to predict the settings and line shapes for the low yield particles. Results are shown in Fig.2 for  $\bar{p}$  and  $d$ . A slightly different technique was used to measure the pion yields. For these measurements the gas refractive index was set to a sufficiently low value that only particles of  $\gamma > 14$  were detected and the Čerenkov counter was used effectively as an integral detector. The pion spectra for momenta greater than 2 Gev/c were taken for one setting of the gas refractive index.

Particles detected by the telescope 1567 were velocity analysed by measurement of their time-of-flight using a time-to-pulse-height converter of the Culligan-Lipman type<sup>15</sup> and the resulting pulse height spectrum was recorded on a 256 channel pulse height analyser. The time-to-pulse-height converter was primed by a 1567 coincidence, started by pulses from the last counter in the beam line (7) and stopped by counter 5. This system, the inverse to that normally used, was adopted because it resulted in the acceptance of fewer random start pulses by the time-to-pulse-height converter, counter 7 having a much lower counting rate than counter 5. The 1567 coincidence circuitry had a resolving time of 12 nsec. The resolution of the time-of-flight system was 1.1 nsec (corresponding to about 12 channels of the pulse-height analyser) which is indicated by the line width observed for fast pions, see Fig.3.

The momentum interval accepted by the spectrometer had a full base width of about 17% and the solid angle was  $5.6 \times 10^{-5}$  sr. The line width for slower particles was greater because of the larger velocity variation corresponding to the momentum spread accepted by the spectrometer. Fig. 3 also shows spectra for 1.6 Gev/c deuterons and 0.8 Gev/c protons.

Measurements were taken with both the Čerenkov and time-of-flight systems for incident proton momenta of 19 and 24 Gev/c. Accidental coincidences and background corresponding to an empty target were measured and gave rise to corrections less than 20%.

### Results

The cross sections found for production of  $\pi^+$ ,  $K^+$ ,  $p^+$  and  $d$  at a laboratory angle of 116 mrad from p-p interactions are given in Tables I and II and are plotted in Figs. 4 - 7. Corrections have been applied for particle decay, absorption, multiple scattering and acceptance of the Čerenkov counter. The acceptance corrections for the Čerenkov counter arose from two causes; firstly, for the lower velocities studied, the momentum acceptance of the counter was less than the momentum accepted by the 1234 counter telescope; and secondly, the anticoincidence arrangement rejected some of the genuine particles. The latter contribution was directly measured and the former was calculated from the counter geometry and the measured response of the Čerenkov counter as a function of gas refractive index for detecting particles of well-defined velocity. Values of these correction factors are given in the tables. The errors quoted include allowances for approximations in the calculations and for uncertainties in the total cross-sections used in computing the absorption corrections. Where no experimental total cross sections were available, geometrical values were used and the deuteron cross-sections were estimated by adding the neutron and proton total cross sections for momenta of half that of the deuteron. The experimental resolution was not in general sufficient to resolve muons or electrons from the pions, but the estimated contamination was less than 10%. The results tabulated and plotted show no errors for uncertainty in the input beam intensity which could be 7% and would scale all results correspondingly.

The agreement between the cross sections measured by the time-of-flight system and the Čerenkov counter is good. Figs. 4 and 5 show the results for 19 GeV/c incident proton momentum and Figs. 6 and 7 for 24 GeV/c. The two latter figures also show the cross sections computed by von Behr and Hagedorn<sup>16</sup> normalised to a total p-p cross section of 40 mb. The computation for deuteron yields was made by Hagedorn<sup>17</sup> using an interaction volume adjusted to give agreement with observed antiproton yields.

The fall in the deuteron cross sections, shown in Figs. 5 and 7, at about 1.5 GeV/c is consistent with it being kinematically impossible to produce deuterons of momenta less than about 1.4 GeV/c for the conditions of this experiment. The average cross section observed below this limit was  $14 \pm 14 \mu\text{b/sr GeV/c}$ .

Table III gives the deuteron cross sections in the centre-of-mass system.

The pion data shown in Fig. 6 includes cross sections for production of  $\pi^0$  deduced by Fidecaro et al.<sup>18</sup> from their  $\gamma$  ray measurements from p-p interactions. The results shown are interpolated from their angular distribution.

Table IV gives the K to  $\pi$  meson ratios found in the present experiment.

## Discussion of Results

### (1) Deuteron Production

This experiment shows conclusively that deuterons are produced with transverse momenta up to 1 GeV/c in high-energy proton-proton collisions.

A comparison of the present results with those of previous experiments is given in Fig. 8 which shows the observed cross sections per nucleon of deuteron production for incident proton momenta of 19-33 GeV/c. It is difficult to compare quantitatively the data because they cover a wide range of angles, incident momenta and target materials but it is obvious that the cross sections reported here for p-p collisions are comparable with other cross sections per nucleon measured with nuclear targets.

It is therefore clear that some of the deuterons observed from a nuclear target originate in nucleon-nucleon collisions, but it is probable that their energy spectra are considerably modified by passage through nuclear matter, the high momentum deuterons being reduced by stripping and the lower momentum deuterons being enhanced by pick-up reactions.

(2) Pion and Proton Production

The  $\pi^+$  yields are greater than the  $\pi^-$  yields, especially at the higher momenta. This is not surprising as the initial particles are both positively charged. The  $\pi^0$  yields<sup>16</sup> (quoted accuracy  $\pm 30\%$ ) are in good agreement with the pion yields reported here (typical accuracy  $\pm 15\%$ ).

Figs. 6 and 7 show that the agreement between the statistically calculated<sup>16,18</sup> and measured laboratory momentum spectra for both pions and protons is poor, particularly at the low momenta where the theoretical spectra decrease very rapidly with the momentum. The theoretical spectra were evaluated by assuming the distribution in the centre-of-mass system to be isotropic. This was an arbitrary simplification adopted to enable spectra in the laboratory system to be easily evaluated.

Acknowledgements

We are grateful to R. Hagedorn for useful discussions and for the computations of deuteron production on the statistical model at 25 GeV/c. Thanks are also due to L. Bird, R. Donnet, P.H. Sharp and C.A. Ståhlbrandt for their assistance. Those of us who were on leave of absence would like to thank the U.K.A.E.A. and N.I.R.N.S. for support.

12.8.1963

Table III Centre-of-mass cross sections for deuteron production at 116 mrad laboratory angle from p-p collisions at 19 and 24 Gev/c.

Proton Momentum Gev/c	Deuteron Momentum (lab)Gev/c	Lab differential cross section $\mu\text{b/sr Gev/c}$	Deuteron Momentum (c.m.s.) Gev/c	Production Angle (c.m.s.) degrees	c.m.s.differential cross section $\mu\text{b/sr Gev/c}$
24	9.20	$11 \pm 5$	1.14	70	$0.7 \pm 0.3$
	6.60	$42 \pm 14$	0.78	102	$2.0 \pm 0.7$
	1.90	$106 \pm 31$	2.55	175	$160 \pm 47$
	1.50	$22 \pm 29$	3.10	177	$60 \pm 80$
19	9.20	$17 \pm 4$	1.25	58	$1.3 \pm 0.3$
	6.30	$47 \pm 15$	0.74	89	$2.1 \pm 0.7$
	1.60	$58 \pm 30$	2.47	176	$110 \pm 57$

Page 117 of 118

11/11/2011 10:11:11 AM

11/11/2011 10:11:11 AM

11/11/2011 10:11:11 AM

11/11/2011 10:11:11 AM

11/11/2011 10:11:11 AM

11/11/2011 10:11:11 AM

11/11/2011 10:11:11 AM

11/11/2011 10:11:11 AM

11/11/2011 10:11:11 AM

11/11/2011 10:11:11 AM

11/11/2011 10:11:11 AM

11/11/2011 10:11:11 AM

11/11/2011 10:11:11 AM

11/11/2011 10:11:11 AM

11/11/2011 10:11:11 AM

11/11/2011 10:11:11 AM

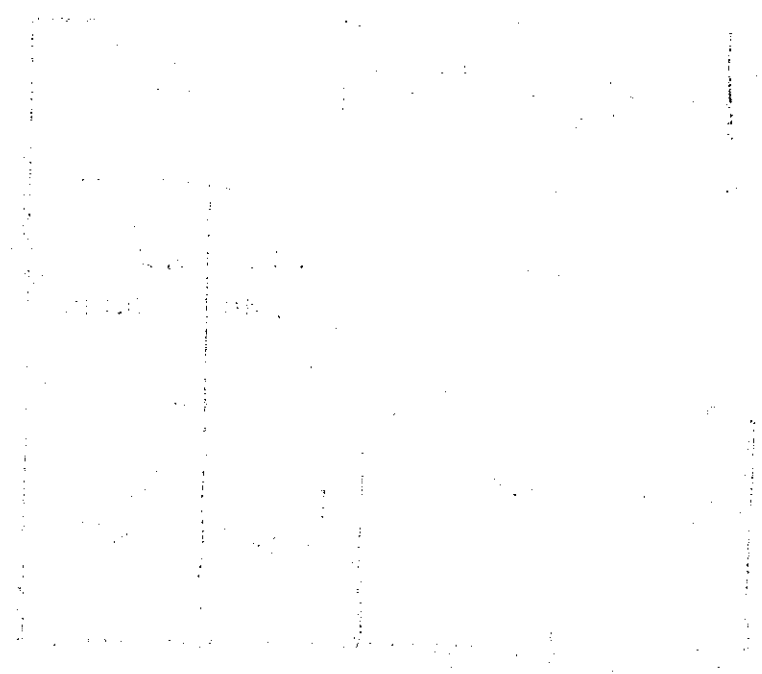
11/11/2011 10:11:11 AM



Table IV K and  $\pi$  meson ratios for 19 Gev/c p-p production at a laboratory angle of 116 mrad

Momentum (lab) Gev/c	$K^+/K^-$	$K^-/\pi^-$	$K^+/\pi^+$
1.70	$2.1 \pm 1.0$	$0.033 \pm$ $0.010$	$0.044 \pm$ $0.011$
2.40	$3.0 \pm 1.0$	$0.036 \pm$ $0.007$	$0.071 \pm$ $0.014$

THE UNIVERSITY OF CHICAGO



## REFERENCES

- \* Permanent address A.E.R.E., Harwell, Berks., England.
- \*\* Permanent address R.H.E.L., Chilton, Didcot, Berks., England
- 1 V.T. Cocconi, T. Fazzini, G. Fidecaro, M. Legros, N.H. Lipman and A.W. Merrison, Phys.Rev.Lett. 5, 19 (1960).
  - 2 G. von Dardel, R. Mermod, G. Weber and K. Winter, Proc. of 1960 Int. Conf. on High-Energy Physics, p. 808.
  - 3 L. Gilly, B. Leontic, A. Lundby, K. Meunier, J.P. Stroot and M. Szeptycka, Proc. of 1960 Int. Conf. on High-Energy Physics, p. 808.
  - 4 V.L. Fitch, S.L. Meyer and P.A. Piroué, Phys.Rev. 126, 1849 (1962).
  - 5 A. Schwarzschild and Č. Zupančič, Phys.Rev. 129, 854 (1963).
  - 6 R. Hagedorn, Phys.Rev.Lett. 5, 276 (1960).
  - 7 S.T. Butler and C.A. Pearson, Phys.Rev.Lett. 7, 69 (1961), Phys.Lett. 1, 77 (1962) and Phys.Rev. 129, 836 (1963).
  - 8 U. Amaldi, Jr., T. Fazzini, G. Fidecaro, G. Ghesquière, M. Legros and H. Steiner, Nuovo Cimento (to be published).
  - 9 E. Balea, E.M. Friedländer, C. Potoceanu and M. Sahini, Nuovo Cimento 25, 214 (1962).
  - 10 G.A. Smith, H. Courant, E.C. Fowler, H. Kraybill, J. Sandweiss and H. Taft, Phys.Rev. 123, 2160 (1961).
  - 11 W.J. Fickinger, E. Pickup, D.K. Robinson and E.O. Salant, Phys.Rev. 125, 2082 (1961).
  - 12 B. Sechi Zorn, Phys.Rev.Lett. 8, 282 (1962) and Bull.Am.Phys.Soc. 7, 349 (1962).
  - 13 D. Harting, J.C. Kluyver and A. Kusumegi, CERN 60-17 (1960).
  - 14 W. Galbraith, G. Manning and A.G. Parham, A.E.R.E. Report R3968 (1962).
  - 15 G. Culligan and N.H. Lipman, Rev.Sci.Inst. 31, 1209 (1960).
  - 16 J. v. Behr and R. Hagedorn, CERN 60-20 (1960).
  - 17 R. Hagedorn, private communication.
  - 18 M. Fidecaro, G. Finocchiaro, G. Gatti, G. Giacomelli, W.A. Middelkoop and T. Yamagata, Nuovo Cimento 24, 73 (1962).

Handwritten text at the top of the page.

Handwritten text below the first line.

Handwritten text below the second line.

Handwritten text below the third line.

Handwritten text below the fourth line.

Handwritten text below the fifth line.

Handwritten text below the sixth line.

Handwritten text below the seventh line.

Handwritten text in the lower middle section.

Handwritten text below the lower middle section.

Handwritten text in the bottom section.

Handwritten text at the very bottom.

## FIGURE CAPTIONS

- Fig. 1 Beam transport system and experimental arrangement. Counters 1, 2, 5, 6 and 7 were 11 cm wide and 10 cm high and counters 3 and 4 were  $7 \times 7 \text{ cm}^2$  and  $6 \times 7 \text{ cm}^2$  respectively.
- Fig. 2 Spectra taken with Čerenkov counter system for a gas refractive index of 1.052 and an incident proton momentum of 19 GeV/c. Filled and open circles represent data taken with full and empty hydrogen target respectively. The line shapes of the  $\bar{p}$  and  $d$  spectra (dashed curves) were obtained from the line shape of the  $p$  spectrum.
- Fig. 3 Time-of-flight spectra for incident proton momentum of 19 GeV/c. Only the deuteron-spectrum has been corrected for background from the empty hydrogen target.
- Fig. 4 Cross sections for the production of  $\pi^+$  and  $K^+$  from p-p collisions at a laboratory angle of 116 mrad and incident proton momentum of 19 GeV/c. Time-of-flight cross sections ( $\blacktriangle \pi^+$ ,  $\triangle \pi^-$ ), Čerenkov counter cross sections ( $\bullet \pi^+$ ,  $\circ \pi^-$ ,  $\blacksquare K^+$ ,  $\square K^-$ ). In the  $\pi^+$  spectra the size of the points indicate the errors. The systematic error of 7% from uncertainties in the input beam intensity has not been included.
- Fig. 5 Cross sections for the production of  $p^+$  and  $d$  from p-p collisions at a laboratory angle of 116 mrad and incident proton momentum of 19 GeV/c. Time-of-flight cross sections ( $\blacktriangle p$ ,  $\blacksquare d$ ), Čerenkov counter cross sections ( $\bullet p$ ,  $\circ \bar{p}$ ,  $\blacksquare d$ ). Where error bars are not shown the size of the points indicate the errors. A systematic error of 7% from uncertainties in the input beam intensity has not been included.
- Fig. 6 Cross sections for the production of  $\pi^+$  from p-p collisions at a laboratory angle of 116 mrad and incident proton momentum of 24 GeV/c. Time-of-flight cross sections ( $\blacktriangle \pi^+$ ,  $\triangle \pi^-$ ), Čerenkov counter cross sections ( $\bullet \pi^+$ ,  $\circ \pi^-$ ). The  $\pi^0$  cross sections shown (symbol X) are interpolated from the results of Fidecaro et al.<sup>18</sup>. The size of the experimental points indicate the errors. The systematic error of 7% from uncertainties in the input beam intensity has not been included. The dashed curve shows results of statistical model calculations<sup>16</sup>.

Fig.7 Cross sections for the production of p and d from p-p collisions at a laboratory angle of 116 mrad and incident proton momentum of 24 Gev/c. Time-of-flight cross sections ( $\blacktriangle$  p,  $\blacksquare$  d), Cerenkov counter cross sections ( $\odot$  p  $\boxtimes$  d). Where error bars are not shown the size of the points indicate the errors. The systematic error of 7% from uncertainties in the input beam intensity has not been included. Curve (a) shows results of statistical model calculations<sup>16</sup> for the production of protons and curve (b) for deuterons<sup>17</sup>.

Fig.8 Summary of deuteron production cross sections per nucleon for incident proton momenta in the range 19 - 33 Gev/c.

(a)	p-Be collisions at 30 Gev/c for 45° laboratory angle (reference 4).
(b)	p-Be " " " " " 90° " " (reference 4).
(c)	p-C " " 26.6 " " 11.25° " " (reference 8).
(d)	p-Be " " 33 " " 13° " " (reference 4).
(e)	p-Al " " 25 " " 16° " " (reference 1).
(f)	p-Be " " 29.5 " " 30° " " (reference 5).
(g)	p-p " " 19+ 24 " " 6.6° " " (this experiment).

Curves (a), (b), (d), (e) and (f) were obtained assuming a target efficiency of 30%.